

Rheology and Ultrasonic Properties of Metallic Glass-Forming Liquids: A Potential Energy Landscape Perspective

William L. Johnson, Marios D. Demetriou,
John S. Harmon, Mary L. Lind,
and Konrad Samwer

Abstract

In the potential energy landscape theory of liquids, the energetic configurational landscape of a liquid is modeled using a potential energy function comprising a population of stable potential energy minima called inherent states, which represent the stable atomic configurations of the liquid. These configurations are separated by saddle points that represent barriers for configurational hopping between the inherent states. In this article, we survey recent progress in understanding metallic glass-forming liquids from a potential energy landscape perspective. Flow is modeled as activated hopping between inherent states across energy barriers that are assumed to be, on average, sinusoidal. This treatment gives rise to a functional relation between viscosity and isoconfigurational shear modulus, leading to rheological laws describing the Newtonian and non-Newtonian viscosity of metallic glass-forming liquids over a broad range of rheological behavior. High-frequency ultrasonic data gathered within the supercooled-liquid region are shown to correlate well with rheological data, thus confirming the validity of the proposed treatment. Variations in shear modulus induced either by thermal excitation or mechanical deformation can be correlated to variations in the measured stored enthalpy or equivalently to the configurational potential energy of the liquid. This shows that the elastic and rheological properties of a liquid or glass are uniquely related to the average potential energy of the occupied inherent states.

Introduction

During the last three decades, the phenomenological theories proposed to explain flow in metallic glasses and liquids can be grouped into two categories: free volume theories¹ and shear transformation zone theories.²

Spaepen introduced the concept of free volume.¹ By drawing an analogy between glassy and granular materials, he proposed that deformation of metallic liquids and glasses is accommodated by the creation of microstructural free volume via a mechanism of flow-induced dilatation. Owing to their ability to effectively replicate the fictive temperature* of the glass, free volume models are capable of simulating the flow characteristics of metallic glasses and liquids and consequently have been widely embraced. Although experimental assessment of excess molar volume by positron annihilation spectroscopy³ and x-ray synchrotron radiation⁴ provided evidence of deformation-induced dilatation, it has not been possible to quantitatively link measurable free volume to flow as predicted from free volume models. This can be attributed to the lack of a fundamental thermodynamic definition of free volume, leading to constitutive models that possibly lack thermodynamic consistency.

Argon, on the other hand, introduced the notion of the shear transformation zones (STZs).² Inspired by the deformation of soap bubble rafts, he proposed that deformation of metallic glasses and liquids is accommodated by plastic rearrangements of atomic regions that involve tens of atoms, termed shear transformation zones (STZs). Experimental evidence gathered from several recent studies⁵⁻⁷ shows that the STZ hypothesis by Argon is consistent with the classical thermodynamic theories of liquids and glasses based on the concept of potential energy landscapes.^{8,9}

In the potential energy landscape theory, a potential energy function is used to model the energetic landscape of the system, which comprises a population of inherent states (basins) associated with local minima that are the stable configurational states of the liquid. These are separated by saddle points that constitute the barriers for configurational hopping between liquid configurations. By assuming the average potential energy versus shear strain in the vicinity of a basin to be a sinusoid, as employed by Frenkel¹⁰

*Fictive temperature is a temperature representing the energy state of the frozen-in glass configuration.

to calculate the theoretical shear strength of a dislocation-free crystal, useful functional relations arise that capture the underlying flow mechanism of metallic glass-forming liquids. In this article, we survey recent progress in understanding metallic glass-forming liquid rheology using a model based on these concepts.

Link between Viscosity and Shear Modulus

Following Frenkel,¹⁰ one can relate the average potential energy density ϕ to the canonical shear strain coordinate γ via

$$\phi/\phi_0 = \sin^2(\pi\gamma/4\gamma_c), \quad (1)$$

where ϕ is the barrier energy density and $4\gamma_c$ is the average configurational spacing. A plot of this function in the vicinity of two inherent states is presented in Figure 1. Here, γ_c is the shear strain limit of the material, which was found to be universal for all known metallic glass systems, taking the value of 0.036 ± 0.002 .⁵ The STZ shear modulus is given by

$$G = d^2\phi/d\gamma^2|_{\gamma=0}, \quad (2)$$

which leads to a linear relationship between barrier energy density and shear modulus as

$$\phi_0 = (8/\pi^2)\gamma_c^2 G. \quad (3)$$

Multiplying by an effective STZ volume Ω , the total energy barrier for configurational hopping between inherent states, which can be regarded as the activation barrier for shear flow, can be expressed as

$$W = (8/\pi^2)\gamma_c^2 G \Omega. \quad (4)$$

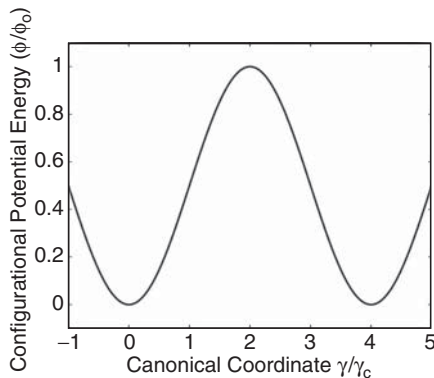


Figure 1. A plot of the potential energy density function $\phi/\phi_0 = \sin^2(\pi\gamma/4\gamma_c)$ in the vicinity of two inherent states; ϕ_0 is the barrier energy density and $4\gamma_c$ is the average configurational spacing.

Noting that the variables determining the barrier height are G and Ω , the expression for the energy barrier can be rearranged as

$$W = W_g(G/G_g)(\Omega/\Omega_g), \quad (5)$$

where G_g is the shear modulus, Ω_g is the STZ volume, and W_g is the flow barrier of the frozen configuration at the glass-transition temperature T_g . While G_g is an experimentally accessible property, Ω_g is not. The flow barrier of the frozen configuration can be expressed as

$$W_g = (8/\pi^2)\gamma_c^2 G_g \Omega_g, \quad (6a)$$

and as will be shown in the following section, it is determined solely by T_g . Its value for most metallic glasses ranges between 2×10^{-19} J and 3×10^{-19} J. Considering a typical value for G_g of 30 GPa, an estimate for the STZ volume can be made as

$$\Omega_g = (\pi^2/8)W_g/(\gamma_c^2 G_g) \approx 5 \text{ nm}^3, \quad (6b)$$

which for a typical atomic volume of 0.02 nm^3 corresponds to ~ 250 atoms.

The seminal variables G and Ω now refer to the shear modulus and STZ volume of the liquid state, respectively. More specifically, G is the average shear modulus of a fixed liquid configuration at temperature T (i.e., averaged over the liquid configurations occupied at temperature T). At T , the occupied inherent states, which constitute the possible liquid configurations, have an average potential energy ε . Both parameters are temperature- and pressure-dependent, $G = G(T, P)$ and $\varepsilon = \varepsilon(T, P)$. For an equilibrium liquid, it follows that G can also be expressed as a function of ε and P : $G = G(\varepsilon, P)$. Similarly, one expects the STZ volume Ω for typical barrier crossing events will depend on T and P : $\Omega = \Omega(T, P)$. Ultrasonic shear wave measurements in the liquid measure this $G(T, P)$, provided that the frequency of the measurement is much higher than the Maxwell relaxation rate of the liquid.^{6,7}

Alternatively, a liquid equilibrated at T and P and configurationally quenched (or frozen) to glass at ambient temperature will give an ambient-temperature shear modulus that reflects the configuration of the liquid at T and P .^{6,7} The configurational potential energy $\varepsilon(T, P)$ of a quenched liquid configuration can likewise be determined by the enthalpy $h(T, P)$, assessed from enthalpy recovery measurements.^{11,12} For a fixed ambient pressure P_0 , the experimental data give

$$\varepsilon(T, P_0) = h(T, P_0), \quad (7)$$

that is, the configurational potential energy is equal to the configurational enthalpy. Combining enthalpy, enthalpy recovery, and ultrasonic measurements, one can determine both $G(T, P_0)$ and $G(\varepsilon, P_0)$ for a glass-forming liquid.

It is the T -dependence (or, equivalently, the ε -dependence) and P -dependence of G and Ω in the liquid that control the barrier height for configurational hopping in the liquid and thus the liquid viscosity. Experiments show that $G(T, P_0)$ falls rapidly with T above the glass-transition temperature, T_g .^{6,13} The functional form of this dependence is discussed in the next sections. The form of $\Omega(T, P_0)$ is experimentally less accessible. One can formally relate these dependencies using the relationship

$$(G/G_g)^n \approx (\Omega/\Omega_g)^p, \quad (8)$$

where the exponents n and p are reduced elastic and STZ volume softening indices, respectively, relating to the rheological character of the liquid in the following paragraphs. Using these indices, the flow barrier in the liquid can be written as

$$W = W_g(G/G_g)^{1/q}, \quad (9)$$

where $q = n/(n+p)$.

Taking the barrier-crossing rate normalized by an attempt frequency to follow a Boltzmann distribution (equivalently, thermally activated hopping), one arrives at a viscosity law that takes the form

$$\frac{\eta}{\eta_\infty} = \exp\left(\frac{W}{kT}\right) = \exp\left[\frac{W_g}{kT} \left(\frac{G}{G_g}\right)^{1/q}\right], \quad (10)$$

where η is the viscosity and η_∞ is the high-temperature (Born-liquid) limit of viscosity, which can be realized in the limit of $W \rightarrow 0$. In analyzing Zr-based⁶ and Pt-based¹³ glass-forming liquids, it was determined that the best correlation between G and η can be obtained when $n \approx p$, that is, $q \approx 1/2$. In the present discussion, we assume $q = 1/2$ to hold for all the liquids considered.

Newtonian Viscosity and Shear Modulus

Newtonian flow can essentially be regarded as thermally activated flow, where barriers are overcome entirely by thermal fluctuations. The Newtonian viscosity would therefore be determined by the shear modulus corresponding to the equilibrium configurational state, G_e , which can be expected to decay with temperature in an approximately exponential

trend. As previously proposed,^{6,7,13} different functions can be employed to describe such decaying behavior, including an exponential decaying law, $\exp(-nT/T_g)$, a power law, $(T_g/T)^n$, or other decaying laws such as $\exp(nT_g/T)$ or $\tanh(nT_g/T)$. In these expressions, n is the elastic softening index identified in the previous section. To maintain consistency with earlier studies,^{7,13} the exponential decaying law will be adopted here:

$$\frac{G_e(T)}{G_g} = \exp\left[n\left(1 - \frac{T}{T_g}\right)\right]. \quad (11)$$

Substituting to Equation 10, the following Newtonian law can be formulated (assuming $q = 1/2$):

$$\frac{\eta_e(T)}{\eta_\infty} = \exp\left\{\frac{W_g}{kT} \exp\left[2n\left(1 - \frac{T}{T_g}\right)\right]\right\}, \quad (12)$$

where k is the Boltzmann constant. The parameter W_g can be determined by requiring Equation 12 to yield the Newtonian viscosity limit at T_g ,

$$\eta_g = \eta_e(T_g) = 10^{12} \text{ Pa s}, \quad (13a)$$

which gives

$$W_g = kT_g \ln(\eta_g/\eta_\infty). \quad (13b)$$

As mentioned in the previous section, η_∞ constitutes the limit of viscosity realized at high temperatures, and in metals can be well approximated by the Planck limit. Therefore, the only unknown variable in the Newtonian law given by Equation 12 is n , and as discussed in earlier studies,^{6,7,13} this variable is related to the fragility of the liquid.[†] The fragility parameter m , as defined by Angell,¹⁴ can be related to n via

$$m = (1 + 2n) \log(\eta_g/\eta_\infty). \quad (14)$$

As recently demonstrated,⁷ by means of the Newtonian viscosity law given by Equation 12, the Newtonian viscosity of metallic glass-forming liquids can be modeled remarkably well for a broad range of fragilities. The Angell plots of low- and high-temperature viscosity data for $\text{Pd}_{77.5}\text{Cu}_6\text{Si}_{16.5}$, $\text{Pd}_{40}\text{Ni}_{40}\text{P}_{20}$, $\text{Zr}_{41.2}\text{Ti}_{13.8}\text{Ni}_{10}\text{Cu}_{12.5}\text{Be}_{22.5}$, and $\text{La}_{55}\text{Al}_{25}\text{Ni}_{20}$, along with the fit of Equation 12, are shown in Figure 2. The fit parameter n and the calculated fragility for each liquid are given

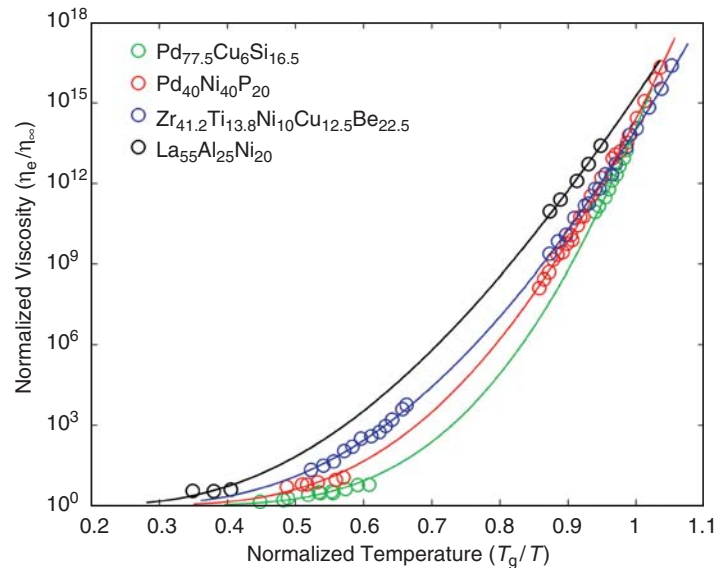


Figure 2. Angell plots of the high- and low-temperature Newtonian viscosity data for several metallic glass-forming liquids, and fit of the equilibrium viscosity law (Equation 12). Experimental viscosity data for these liquids are taken from the literature.^{7,18,23}

in Table I. It is interesting to note that the one-parameter law presented here is capable of capturing Newtonian data more accurately than the two most widely adopted viscosity laws: the two-parameter Vogel–Fulcher–Tammann law¹⁵ and the three-parameter Cohen–Grest law.¹⁶

The basis of the new viscosity law rests on the argument that viscosity should be related to shear modulus through the activation barrier for configurational hopping between the inherent states of the potential energy landscape. We have validated this argument by using Equation 10 to correlate the Newtonian viscosity data of various liquids to equilibrium high-frequency shear modulus data assessed from ultrasonic measurements for the liquid at varying temperature. Reported shear modulus data for

$\text{Pt}_{57.5}\text{Ni}_{5.3}\text{Cu}_{14.7}\text{P}_{22.5}$,¹³ $\text{Pd}_{43}\text{Ni}_{10}\text{Cu}_{27}\text{P}_{20}$,¹⁷ and $\text{Zr}_{46.25}\text{Ti}_{8.25}\text{Ni}_{10}\text{Cu}_{7.5}\text{Be}_{27.5}$,⁶ are shown in Figure 3. The data are fitted to an exponential decaying law using Equation 11. The fits are presented in Figure 3, while the fitting parameters n and interpolated parameters T_g and G_g are listed in Table II. Using reported Newtonian viscosity data for $\text{Pt}_{57.5}\text{Ni}_{5.3}\text{Cu}_{14.7}\text{P}_{22.5}$,¹¹ $\text{Pd}_{43}\text{Ni}_{10}\text{Cu}_{27}\text{P}_{20}$,^{7,18} and $\text{Zr}_{46.25}\text{Ti}_{8.25}\text{Ni}_{10}\text{Cu}_{7.5}\text{Be}_{27.5}$,¹⁹ one can use Equation 10 to determine a corresponding shear modulus. The rheological shear moduli determined from measured viscosity data (Figure 3) overlay onto the ultrasonic shear modulus data very well, verifying that Newtonian viscosity has a unique functional relationship and a one-to-one correspondence with the equilibrium liquid shear modulus.

Table I: Fit Parameters to the Newtonian Viscosity Law.

Metallic Glass-Forming Liquid	η_∞ (Pa s)	T_g (K)	Fit Parameter, n	Fragility Parameter, m
$\text{Pd}_{77.5}\text{Cu}_6\text{Si}_{16.5}$	7.7×10^{-3}	634	1.663	61
$\text{Pd}_{40}\text{Ni}_{40}\text{P}_{20}$	3.7×10^{-3}	560	1.241	50
$\text{Zr}_{41.2}\text{Ti}_{13.8}\text{Ni}_{10}\text{Cu}_{12.5}\text{Be}_{22.5}$	9.3×10^{-3}	613	0.930	40
$\text{La}_{55}\text{Al}_{25}\text{Ni}_{20}$	5.2×10^{-4}	450	0.715	37

Note: Fit parameters to the equilibrium viscosity law for four metallic glass-forming liquids of varying fragility. The reported glass-transition temperature T_g is the interpolated value for which $\eta_g \equiv 10^{12}$ Pa s, while the high-temperature limit of viscosity η_∞ is a value near the Planck limit that resulted in a best fit (as typically implemented when fitting viscosity).

[†]The fragility of a liquid is defined by Angell¹⁴ as the steepness of the viscosity temperature-dependence in the vicinity of the glass transition.

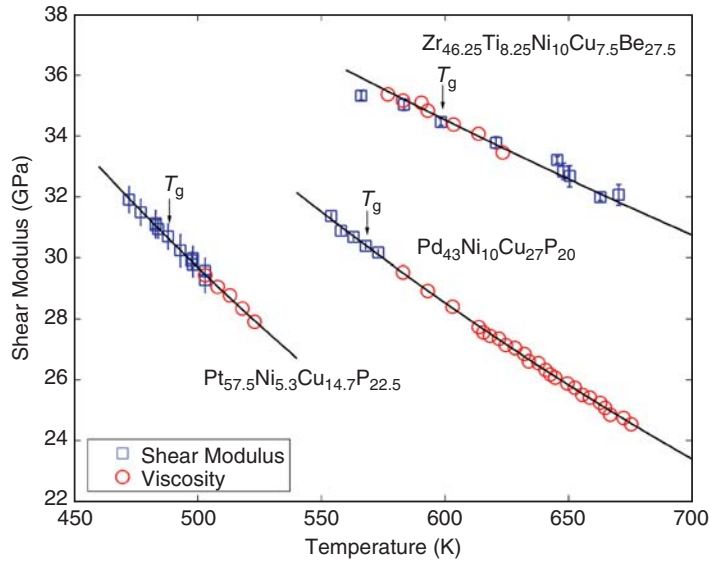


Figure 3. Equilibrium shear modulus data (with associated error bars) measured ultrasonically for Pt-based,^{9,13} Pd-based,¹⁷ and Zr-based^{6,19} glass-forming liquids, shown with Newtonian viscosity data converted to shear modulus via Equation 10. Fits of the equilibrium shear modulus law (Equation 11) are also presented.

Table II: Fit Parameters to the Non-Newtonian Viscosity Law.

Metallic Glass-Forming Liquid	η_{∞} (Pa s)	T_g (K)	G_g (GPa)	Fit Parameter, n	α
Pt _{57.5} Ni _{5.3} Cu _{14.7} P _{22.5}	4.5×10^{-5}	489	30.5	1.290	39.2
Pd ₄₃ Ni ₁₀ Cu ₂₇ P ₂₀	5.1×10^{-5}	567	30.4	1.128	45.9
Zr _{46.25} Ti _{8.25} Ni ₁₀ Cu _{7.5} Be _{27.5}	4.0×10^{-5}	597	34.7	0.693	...
Zr _{41.2} Ti _{13.8} Ni ₁₀ Cu _{12.5} Be _{22.5}	9.3×10^{-3}	613	33.2	0.930	16.2

Note: Parameters for the equilibrium and nonequilibrium viscosity and shear modulus laws to fit data for Pt-based, Pd-based, and Zr-based glass-forming liquids in the vicinity of the glass-transition temperature T_g . α is an unknown parameter in Equation 19 quantifying the deviation of the system's relaxation rate from Maxwellian. No α value for Zr_{46.25}Ti_{8.25}Ni₁₀Cu_{7.5}Be_{27.5} is reported, since its non-Newtonian viscosity has not been investigated. Also, due to the lack of high-temperature Newtonian viscosity data for Pt_{57.5}Ni_{5.3}Cu_{14.7}P_{22.5}, Pd₄₃Ni₁₀Cu₂₇P₂₀, and Zr_{46.25}Ti_{8.25}Ni₁₀Cu_{7.5}Be_{27.5} liquids, the high-temperature limit of viscosity η_{∞} is taken to be the Planck limit. G_g is the shear modulus of the frozen configuration at T_g .

Non-Newtonian Viscosity and Shear Modulus

The proposed barrier softening law, Equation 10, was extended to the case of a driven (nonequilibrium) system.⁷ A non-Newtonian flow law can be formulated by assuming that the irreversible barrier-crossing events are associated with a flow-induced shift in the configurational state and its potential energy ϵ with consequent softening of W . The rate of barrier softening can be formulated as

$$\dot{W}_{\text{sof}} = \dot{\epsilon} \delta W / \delta \epsilon, \quad (15)$$

where $\dot{\epsilon} \propto \eta \dot{\gamma}^2$ is the rate of dissipated mechanical energy density ($\dot{\gamma}$ is the strain

rate), which at steady-state can be taken to be equivalent to the production rate of specific configurational potential energy density. Meanwhile,

$$\delta W / \delta \epsilon = (\partial W / \partial T) / (\partial \epsilon / \partial T) \quad (16)$$

is a thermodynamic parameter denoting changes in W with respect to changes in ϵ . Near T_g ,

$$\partial W / \partial \epsilon \approx -2nW_g / T_g \Delta c_p, \quad (17)$$

where Δc_p is the specific heat capacity change at T_g associated with configurational excitation of inherent states in the liquid. The rate of configurational relax-

ation is then formulated by assuming the irreversible barrier-crossing events to be unimolecular Maxwellian relaxation processes:

$$\dot{W}_{\text{rel}} = (W - W_e) / \alpha \tau_M, \quad (18a)$$

where

$$W_e(T) = W_g \exp[2n(1 - T/T_g)] \quad (18b)$$

is the equilibrium barrier energy density, α is an unknown parameter quantifying the deviation of the system's relaxation rate from Maxwellian, and

$$\tau_M = \eta / G = \eta / \left[G_g (W/W_g)^{1/2} \right] \quad (18c)$$

is the Maxwell relaxation time. Requiring $\dot{W}_{\text{sof}} = \dot{W}_{\text{rel}}$ for steady flow, a self-consistent nonequilibrium law has been obtained:

$$-\alpha \frac{2nW_g}{T_g \Delta c_p} \eta \dot{\gamma}^2 = \frac{(W - W_e)(W/W_g)^{1/2}}{\eta / G_g}. \quad (19)$$

Using Equation 19, the non-Newtonian viscosity of metallic glass-forming liquids can be modeled remarkably well over a broad range of strain rates. The non-Newtonian data for Pt_{57.5}Ni_{5.3}Cu_{14.7}P_{22.5},⁹ Pd₄₃Ni₁₀Cu₂₇P₂₀,⁷ and Zr_{41.2}Ti_{13.8}Ni₁₀Cu_{12.5}Be_{22.5},²⁰ are shown in Figure 4. The experimental parameters η_{∞} , T_g , G_g , and the fitting parameters n (obtained from Figure 3) used for these liquids are listed in Table II, while the measured Δc_p is listed in Table III. The nonequilibrium law, Equation 19, is fitted to the non-Newtonian data by adjustment of only one parameter, α , where n was already determined by the Newtonian viscosity fits (Figure 3). The fits to the data are presented in Figure 4, and the optimized values of α are listed in Table II. As can be seen, the nonequilibrium law effectively describes the non-Newtonian viscosity of liquids by adjustment of only one additional parameter.

As with the Newtonian law, the non-Newtonian law can be validated by correlating the non-Newtonian viscosity data to the nonequilibrium shear modulus via Equation 10. We have utilized nonequilibrium shear modulus data for Pt_{57.5}Ni_{5.3}Cu_{14.7}P_{22.5},¹³ Pd₄₃Ni₁₀Cu₂₇P₂₀,⁷ and Zr_{41.2}Ti_{13.8}Ni₁₀Cu_{12.5}Be_{22.5},⁷ measured ultrasonically on specimens deformed at constant strain rate and T and then quenched. The results are shown in Figure 5. The data are fitted using Equation 4 in conjunction with Equation 10 and by using the optimized α values listed in Table II. We also used non-Newtonian viscosity data for Pt_{57.5}Ni_{5.3}Cu_{14.7}P_{22.5},⁹ Pd₄₃Ni₁₀Cu₂₇P₂₀,⁷ and

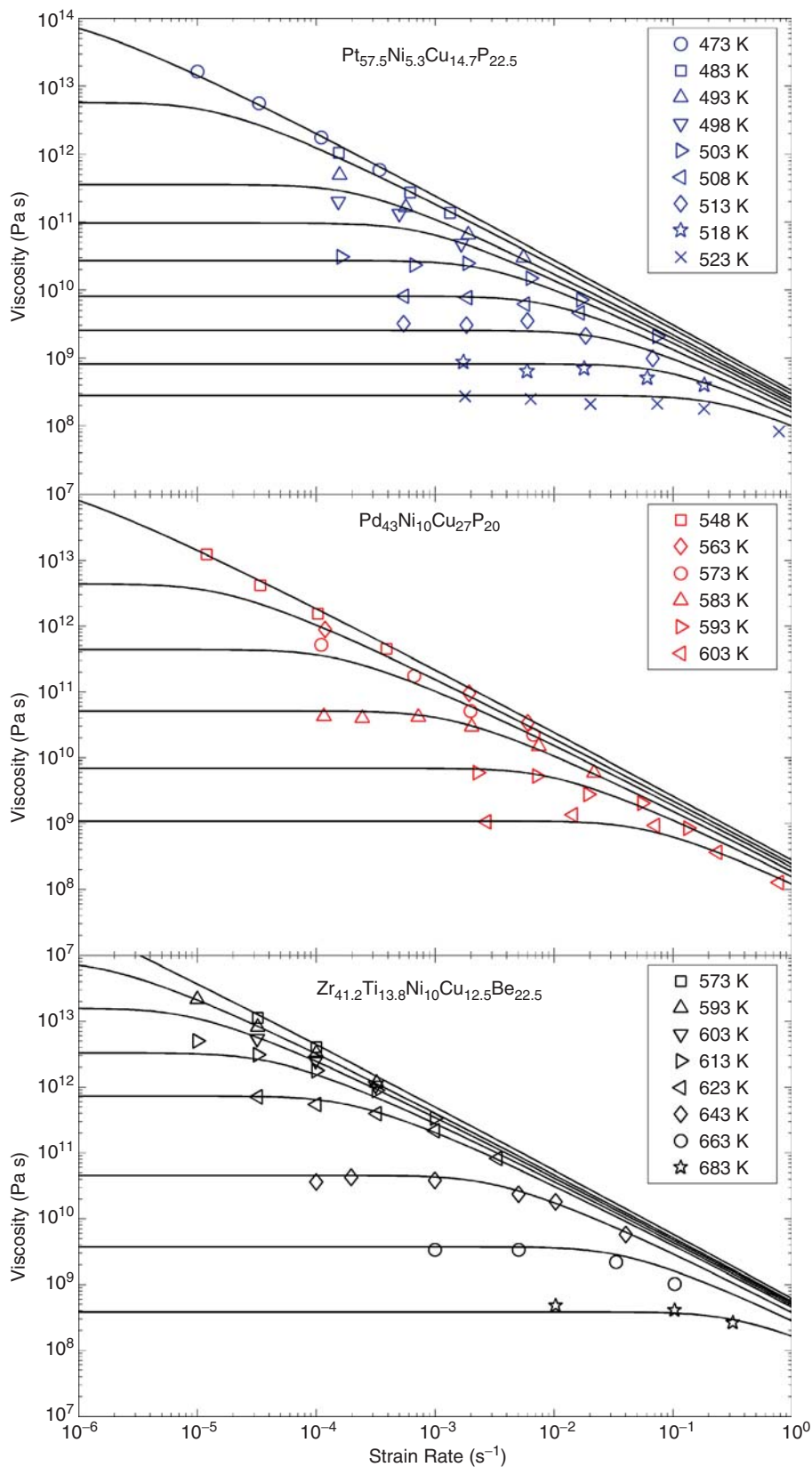


Figure 4. Fit of the nonequilibrium viscosity law, Equation 19, to the non-Newtonian data of (top) Pt-based,⁹ (center) Pd-based,⁷ and (bottom) Zr-based²⁰ glass-forming liquids.

Zr_{41.2}Ti_{13.8}Ni₁₀Cu_{12.5}Be_{22.5},²⁰ which we converted into shear modulus using Equation 10, and superimposed them onto the shear modulus data of Figure 5. The correlated non-Newtonian viscosity data are shown to overlay onto the shear modulus data remarkably well, hence validating that the relationship between viscosity and shear modulus holds for driven systems as well.

Dependence of Shear Modulus on Configurational Potential Energy

So far, it was demonstrated that variations in viscosity with both temperature and strain rate can be uniquely correlated to variations in isoconfigurational shear modulus and hence verified that viscosity has a unique functional relationship and a one-to-one correspondence with shear modulus. This viscosity–shear modulus relationship implies that softening of metallic glass-forming liquids induced by either thermal excitation (by varying temperature) or mechanical deformation (by varying strain rate) is governed by the dependence of isoconfigurational shear modulus on configurational potential energy. As recently demonstrated,¹² softening of metallic glass-forming liquids is indeed governed by a unique functional relationship between shear modulus and configurational potential energy. Such relationship arises directly from the potential energy landscape theory and has been validated by recent molecular dynamics simulations.^{21,22}

The change in the shear modulus induced by thermal annealing near T_g with respect to changes in configurational potential energy can be determined as

$$\left(\frac{dG}{d\Delta h}\right)_{\text{th}} \equiv \left(\frac{dG_e}{dT}\right)_{T_g} / \Delta C_p, \quad (20)$$

where $\left(\frac{dG_e}{dT}\right)_{T_g}$ is the slope of the temperature-dependent equilibrium shear modulus at T_g . One can estimate $\left(\frac{dG_e}{dT}\right)_{T_g}$ for each of the liquids presented in Figure 3 by performing a linear regression to the ultrasonic data. The calculated $\left(\frac{dG}{d\Delta h}\right)_{\text{th}}$ for each liquid is given in Table III.

For each liquid, we can compare $\left(\frac{dG}{d\Delta h}\right)_{\text{th}}$ realized by thermal excitation to $\left(\frac{dG}{d\Delta h}\right)_{\text{me}}$ realized by mechanical deformation. The change in configurational potential energy during steady-state deformation can be assessed by means of enthalpy recovery measurements, as discussed earlier. Enthalpy recovery measurements were performed on deformed Pt_{57.5}Ni_{5.3}Cu_{14.7}P_{22.5},¹² Pd₄₃Ni₁₀Cu₂₇P₂₀,¹² and Zr_{46.25}Ti_{8.25}Ni₁₀Cu_{7.5}Be_{27.5}¹⁷ specimens for which ultrasonic data were previously

Table III: Relationship between Calorimetric and Ultrasonic Data.

Metallic Glass-Forming Liquid	Specific Heat Capacity Change, Δc_p (MJ/m ³ K)	dG_g/dT^a (MPa/K)	$(dG/d\Delta h) _{th}^b$	$(dG/d\Delta h) _{me}^c$
Pt _{57.5} Ni _{5.3} Cu _{14.7} P _{22.5}	2.56	-80	-31.2	-31.0
Pd ₄₃ Ni ₁₀ Cu ₂₇ P ₂₀	2.50	-60	-24.0	-22.7
Zr _{46.25} Ti _{8.25} Ni ₁₀ Cu _{7.5} Be _{27.5}	1.70	-35	-20.6	...
Zr _{41.2} Ti _{13.8} Ni ₁₀ Cu _{12.5} Be _{22.5}	1.50	-17.2

Note: Relationship between calorimetric and ultrasonic data gathered for Pt-based, Pd-based, and Zr-based glass-forming liquids in the vicinity of T_g . No $(dG/d\Delta h)|_{me}$ value for Zr_{46.25}Ti_{8.25}Ni₁₀Cu_{7.5}Be_{27.5} is reported, since its nonequilibrium shear modulus has not been investigated. Also, no $(dG/d\Delta h)|_{th}$ value for Zr_{41.2}Ti_{13.8}Ni₁₀Cu_{12.5}Be_{22.5} is reported, since its equilibrium shear modulus has not been investigated.

^a dG_e/dT is the change of the equilibrium G with respect to T at T_g , and is evaluated from the ultrasonic data gathered at different temperatures.

^b $(dG/d\Delta h)|_{th}$ is the change of G with respect to Δh realized by thermal excitation, and is evaluated using Equation 20.

^c $(dG/d\Delta h)|_{me}$ is the change of G with respect to Δh realized by mechanical deformation, and is evaluated from ultrasonic data gathered at different strain rates and the associated enthalpy recovery data.

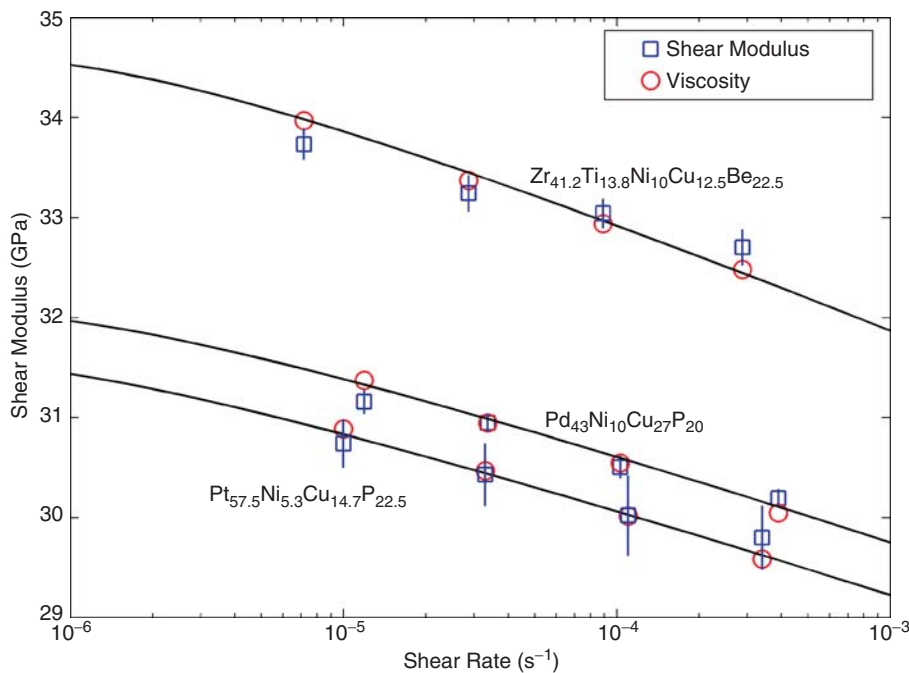


Figure 5. Nonequilibrium shear modulus data (with associated error bars) measured acoustically for Pt-based,^{9,13} Pd-based,⁷ and Zr-based^{7,20} glass-forming liquids, shown together with non-Newtonian viscosity data converted to shear modulus via Equation 10. Fits of the nonequilibrium law, Equation 19, are also presented.

obtained. In Figure 6, the shear modulus of the deformed specimens measured ultrasonically is plotted against the change in stored enthalpy assessed by differential scanning calorimetry data for the three liquids considered. We can estimate $(dG/d\Delta h)|_{me}$ for each of the liquids by

performing a linear regression to the data. The calculated $(dG/d\Delta h)|_{me}$ for each liquid is presented in Table III.

By comparing $(dG/d\Delta h)|_{th}$ to $(dG/d\Delta h)|_{me}$ for each liquid in Table III, we notice that the corresponding values are equal within experimental error. It should be noted that

even though Zr_{46.25}Ti_{8.25}Ni₁₀Cu_{7.5}Be_{27.5} and Zr_{41.2}Ti_{13.8}Ni₁₀Cu_{12.5}Be_{22.5} are essentially different variations of the same alloy family, $(dG/d\Delta h)|_{th}$ for Zr_{46.25}Ti_{8.25}Ni₁₀Cu_{7.5}Be_{27.5} compares well with $(dG/d\Delta h)|_{me}$ of Zr_{41.2}Ti_{13.8}Ni₁₀Cu_{12.5}Be_{22.5}. This equivalence can be illustrated graphically by superimposing the plot of $(dG/d\Delta h)|_{th}$ onto the respective data for each liquid, as shown in Figure 6. It has therefore been demonstrated that softening of metallic glass-forming liquids induced by either thermal excitation or mechanical deformation is governed by a unique functional relationship between shear modulus and specific configurational potential energy of the corresponding liquid inherent states.

Concluding Remarks

The new rheological model described here is properly termed a “cooperative shear model.” It provides a simple description of the average height of the barriers that separate the stable configurations of a liquid in terms of a single configurational coordinate, the macroscopic shear strain imposed on the liquid. The barrier energy density is taken to have a simple sinusoidal form, which gives rise to a relationship linking the barrier energy density to the isoconfigurational shear modulus G and the critical shear strain at the barrier. This critical shear strain has been found to be universal for all metallic glasses studied, taking the value of

$$2\gamma_c = 2 \times 0.036 = 0.072. \quad (21)$$

As such, the elastic energy density at the barrier depends on a single parameter, the experimentally measurable liquid shear modulus. The absolute barrier heights for cooperatively shearing STZs, which determine the liquid viscosity, are also proportional to the effective volume Ω of the corresponding STZ (i.e., the region of cooperativity). By recognizing a functional interdependence between G and Ω , a rheological law has been formulated that uniquely relates the absolute barrier height for cooperative shearing to the measurable isoconfigurational shear modulus.

This new rheological law provides a consistent description of both the Newtonian and non-Newtonian viscosity of metallic glass-forming liquids over a broad range of fragility. The model has been experimentally validated by demonstrating that high-frequency ultrasonic measurements of the liquid G as a function of temperature and strain rate are directly correlated to the measured liquid viscosity. It was also demonstrated that variations in shear modulus induced by either thermal excitation (Newtonian

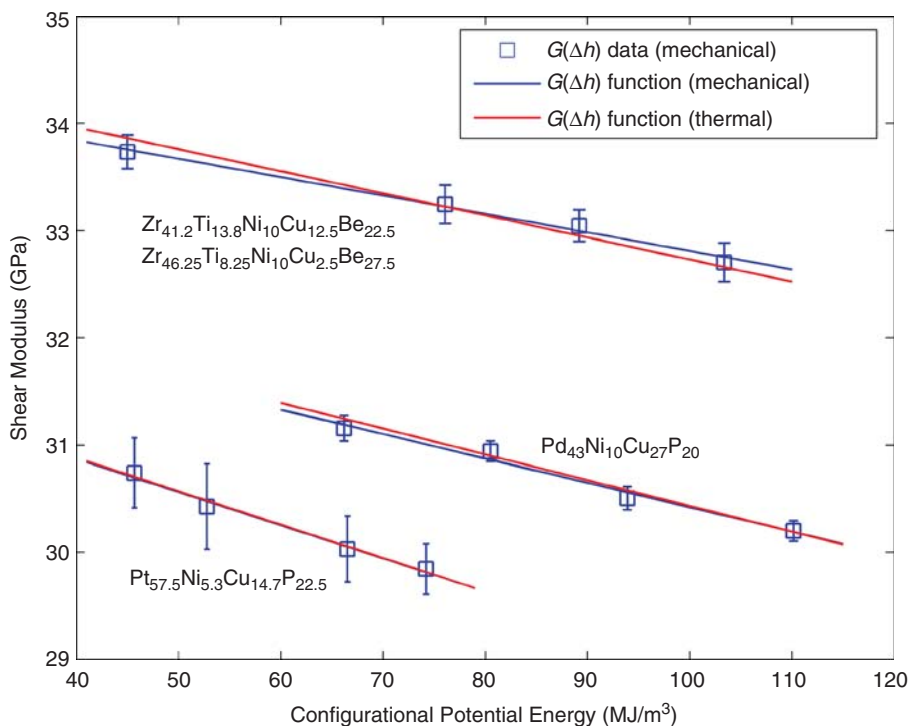


Figure 6. $G(\Delta h)$ data (mechanical): Variations in nonequilibrium shear modulus induced by mechanical deformation plotted against changes in stored enthalpy for Pt-based,^{12,13} Pd-based,^{12,17} and Zr-based^{6,7,17} glass-forming liquids. $G(\Delta h)$ function (mechanical): Functional relations governing variations in nonequilibrium shear modulus with respect to changes in stored enthalpy induced by mechanical deformation (fit to the data). $G(\Delta h)$ function (thermal): Functional relations governing variations in equilibrium shear modulus with respect to changes in stored enthalpy induced by thermal excitation (from Equation 20).

viscosity at varying liquid temperature) or mechanical deformation (non-Newtonian viscosity at fixed temperature and varying strain rate) are uniquely related to variations in the stored specific enthalpy of the liquid. It is thus established that the softening of G (with temperature and strain rate) in these materials is governed primarily by the dependence of the shear modulus on the specific enthalpy (or potential energy) of the liquid configuration. Both G and the height of the flow barriers separating occupied liquid inherent states decrease systematically and predictably with increasing potential energy

of these occupied inherent states. In summary, the new model reveals simple relations between liquid rheology and average features of the potential energy landscape.

References

1. F. Spaepen, *Acta Metall.* **25**, 407 (1977).
2. A.S. Argon, *Acta Metall.* **27**, 47 (1979).
3. K.M. Flores, D. Suh, R.H. Dauskardt, P. Asoka-Kumar, P.A. Sterne, R.H. Howell, *J. Mater. Res.* **17**, 1153 (2002).
4. K. Hajlaoui, T. Benameur, G. Vaughan, A.R. Yavari, *Scripta Mater.* **51**, 843 (2004).
5. W.L. Johnson, K. Samwer, *Phys. Rev. Lett.* **95**, 195501 (2005).

6. M.L. Lind, G. Duan, W.L. Johnson, *Phys. Rev. Lett.* **97**, 015501 (2006).
7. M.D. Demetriou, J.S. Harmon, M. Tao, G. Duan, K. Samwer, W.L. Johnson, *Phys. Rev. Lett.* **97**, 065502 (2006).
8. F.H. Stillinger, T.A. Weber, *Science* **267**, 1935 (1995).
9. P.G. Debenedetti, F.H. Stillinger, *Nature* **410**, 259 (2001).
10. J. Frenkel, *Z. Phys.* **37**, 572 (1926).
11. R. Busch, W.L. Johnson, *Appl. Phys. Lett.* **72**, 2695 (1998).
12. J.S. Harmon, M.D. Demetriou, W.L. Johnson, *Appl. Phys. Lett.* **90**, 131912 (2007).
13. J.S. Harmon, M.D. Demetriou, W.L. Johnson, *Appl. Phys. Lett.* **90**, 171923 (2007).
14. C.A. Angell, *J. Non-Cryst. Solids* **73**, 1 (1985).
15. H. Vogel, *Z. Phys.* **22**, 645 (1921); G.S. Fulcher, *Am. Ceram. Soc. Bull.* **8**, 339 (1925); G. Tammann, G. Hesse, *Z. Anorg. Allg. Chem.* **156**, 245 (1926).
16. M.H. Cohen, G.S. Grest, *Phys. Rev. B: Condens. Matter* **20**, 1077 (1979).
17. J.S. Harmon, PhD thesis, California Institute of Technology (2007).
18. G.H. Fan, H.-J. Fecht, E.J. Lavernia, *Appl. Phys. Lett.* **84**, 487 (2004).
19. R. Busch, E. Bakke, W.L. Johnson, *Acta Mater.* **46**, 4725 (1998).
20. J. Lu, G. Ravichandran, W.L. Johnson, *Acta Mater.* **51**, 3429 (2003).
21. G. Duan, M.L. Lind, M.D. Demetriou, W.L. Johnson, W.A. Goddard III, T. Cagin, K. Samwer, *Appl. Phys. Lett.* **89**, 151901 (2006).
22. M. Zink, K. Samwer, W.L. Johnson, S.G. Mayr, *Phys. Rev. B: Condens. Matter* **74**, 012201 (2006).
23. A. Masuhr, T.A. Waniuk, R. Busch, W.L. Johnson, *Phys. Rev. Lett.* **82**, 2290 (1999); K.H. Tsang, S.K. Lee, H.W. Kui, *J. Appl. Phys.* **70**, 4837 (1991); G. Wilde, G.P. Görlner, K. Jeropoulos, R. Willnecker, H.-J. Fecht, *Mater. Sci. Forum* **269-272**, 541 (1998); Y. Kawamura, A. Inoue, *Appl. Phys. Lett.* **77**, 1114 (2000); H.S. Chen, *J. Non-Cryst. Solids* **27**, 257 (1978); I. Egry, G. Lohofer, I. Seyhan, S. Schneider, B. Feuerbacher, *Int. J. Thermophys.* **20**, 1005 (1999); Y. Kawamura, T. Nakamura, H. Kato, H. Mano, A. Inoue, *Mater. Sci. Eng. A* **304-306**, 674 (2001); T. Yamasaki, T. Tatibana, Y. Ogino, A. Inoue, in *Bulk Metallic Glasses*, W.L. Johnson, A. Inoue, C.T. Liu, Eds. (Mater. Res. Soc. Symp. Proc. **554**, Warrendale, PA, 1999) p. 63. □

The Materials Research Society proudly introduces the...

MRS FELLOW PROGRAM

Honoring outstanding individuals from around the world who are notable for their sustained and distinguished contributions to the advancement of materials research

For details visit:
www.mrs.org/fellow

